

## VU Research Portal

### XUV-LASER SPECTROSCOPY ON CO - ISOTOPE-SELECTIVE PREDISSOCIATION RATES

Levelt, P.F.; Ubachs, W.M.G.; Hogervorst, W.

**published in**

Journal de physique II  
1992

**DOI (link to publisher)**

[10.1051/jp2:1992167](https://doi.org/10.1051/jp2:1992167)

**document version**

Publisher's PDF, also known as Version of record

[Link to publication in VU Research Portal](#)

**citation for published version (APA)**

Levelt, P. F., Ubachs, W. M. G., & Hogervorst, W. (1992). XUV-LASER SPECTROSCOPY ON CO - ISOTOPE-SELECTIVE PREDISSOCIATION RATES. *Journal de physique II*, 2(4), 801-812.  
<https://doi.org/10.1051/jp2:1992167>

**General rights**

Copyright and moral rights for the publications made accessible in the public portal are retained by the authors and/or other copyright owners and it is a condition of accessing publications that users recognise and abide by the legal requirements associated with these rights.

- Users may download and print one copy of any publication from the public portal for the purpose of private study or research.
- You may not further distribute the material or use it for any profit-making activity or commercial gain
- You may freely distribute the URL identifying the publication in the public portal ?

**Take down policy**

If you believe that this document breaches copyright please contact us providing details, and we will remove access to the work immediately and investigate your claim.

**E-mail address:**

[vuresearchportal.ub@vu.nl](mailto:vuresearchportal.ub@vu.nl)

Classification

Physics Abstracts

33.20N — 33.80G — 98.40C

## XUV-laser spectroscopy on CO: isotope-selective predissociation rates

Pieternel F. Levelt, Wim Ubachs and Wim Hogervorst

Laser Centre Free University, Department of Physics and Astronomy, De Boelelaan 1081, 1081 HV Amsterdam, The Netherlands

(Received 5 November 1991, accepted 18 December 1991)

**Abstract.** — The K ( $4p\sigma$ )  $^1\Sigma^+$ ,  $v = 0$  and W ( $3s\sigma$ )  $^1\Pi$ ,  $v = 2$  states in  $^{12}\text{C}^{16}\text{O}$  and  $^{13}\text{C}^{16}\text{O}$  have been studied in high resolution with extreme ultraviolet laser radiation in the wavelength range 94 – 97 nm. Accurate spectroscopic constants for both isotopes and states have been derived from absolute rotational line positions. From linewidths of individual rotational transitions predissociation rates for  $^{12}\text{C}^{16}\text{O}$  and  $^{13}\text{C}^{16}\text{O}$  in the W  $^1\Pi$   $v = 2$  state have been deduced:  $k_p(^{12}\text{CO}) = 1.15 (15) \times 10^{11} \text{ s}^{-1}$  and  $k_p(^{13}\text{CO}) = 0.58 (13) \times 10^{11} \text{ s}^{-1}$ . The rate of photodissociation of K  $^1\Sigma^+$ ,  $v = 0$  was found to be smaller:  $k_p = 2.6 (1.3) \times 10^{10} \text{ s}^{-1}$  for both isotopes.

### 1. Introduction.

After molecular hydrogen, carbon monoxide is the most abundant molecule in interstellar clouds and circumstellar envelopes. By virtue of its permanent electric dipole moment purely rotational transitions are readily detectable in radio-astronomy. CO is considered to be the monitoring probe for chemical dynamics in these regions of outer space. However, the rotational emission lines of  $^{12}\text{C}^{16}\text{O}$  tend to saturate at high column densities, so spectroscopic and dynamical information on other isotopic combinations is required to map out CO densities. The main destruction mechanism for CO in the outer spatial regions considered is photodissociation induced by stellar radiation. Through a large number of recent theoretical and experimental investigations [1-6] it has been established that:

(i) the wavelength range between  $\lambda = 91.2$  nm (continuum absorption of atomic hydrogen) and  $\lambda = 111.8$  nm (corresponding to the dissociation limit of CO) is particularly important for the decomposition of CO;

(ii) photodissociation takes place predominantly through predissociation of bound states and not via direct dissociation through continuum states. Some evidence for isotope-dependent predissociation rates has been found [3];

(iii) coincidental shielding effects by absorption lines of H and  $\text{H}_2$  as well as mutual shielding of different isotopes of CO play an important role [2].

So high resolution spectroscopic studies on the highly excited states of carbon monoxide in the energy range 11.1 – 13.6 eV are required. According to Stark *et al.* [5], there is a need to determine accurately line assignments, photoabsorption coefficients and predissociation probabilities. This to fully understand the abundance, excitation and isotopic fractionation of CO in interstellar clouds and in circumstellar envelopes.

Different techniques have been employed in the laboratory to map out the spectroscopy and dynamics of the excited states of CO which have astrophysical relevance. With synchrotron radiation the CO molecule has been investigated in the range 91 – 115 nm with intermediate resolution [4] revealing the vibronic band structure. These bands have been resolved for rotational structure in a number of extreme ultraviolet (XUV) absorption studies using synchrotron radiation [5] or a classical 10 m vacuum spectrograph [3] with a resolution down to  $0.5 \text{ cm}^{-1}$ . Lasers have been used in three-color multistep excitation [7] and in one-color (2 + 1) multi-photon ionization [8]. An alternative approach for the study of highly excited states of CO by means of laser excitation is the technique of optogalvanic spectroscopy in hollow cathode discharges. Masaki *et al.* [9] investigated the  $K^1\Sigma^+$ ,  $v = 0$  state in one-photon excitation from the discharge populated  $B^1\Sigma^+$  state.

In the present investigation a narrow-band extreme ultraviolet laser spectrometer was used for high resolution excitation studies of the  $K^1\Sigma^+ - X^1\Sigma^+ (0,0)$  and  $W^1\Pi - X^1\Sigma^+ (2,0)$  bands of CO in the wavelength range 96.97 – 97.12 nm and 94.11 – 94.17 nm respectively. Both bands were studied for  $^{12}\text{CO}$  as well as for  $^{13}\text{CO}$ , with the highest spectral resolution achieved thusfar. Furthermore, in the nonlinear optical conversion process generating coherent XUV radiation, exact harmonics are produced. This allows for a calibration against the  $I_2$ -frequency standard in the visible resulting in an absolute accuracy of  $0.04 \text{ cm}^{-1}$  on unblended CO rotational transitions. From observed line widths of these transitions accurate predissociation rates were deduced for the  $W^1\Pi v = 2$  state. Different predissociation rates are found for  $^{12}\text{CO}$  and  $^{13}\text{CO}$  in this particular state.

## 2. Experiment.

The XUV laser spectrometer was composed of a pump and dye laser combination, and a high-vacuum setup consisting of three differentially pumped chambers. The extreme ultraviolet (XUV) radiation was generated in the first chamber. Here the third harmonic of ultraviolet (UV) laser light was produced in a free jet of Xenon gas. The UV light was focused by a 20 cm lens close to the orifice of a piezo-electrically driven pulsed valve. The generated XUV and the UV light passed through a pinhole into a second chamber, the detection chamber. Attached to this detection chamber was a third chamber, containing a solenoid pulsed valve. A supersonically cooled CO beam (neat CO gas) was produced, passing a skimmer before entering the detection chamber. Here the diverging XUV and UV beam (diameter 1.5 cm) intersected the CO molecular beam. It was also possible to produce a molecular beam with a near room temperature population distribution by adjusting the time delay of the laser pulse (such that excitation occurs in a hot tail of the gas pulse). An extensive description of the XUV laser spectrometer will be published elsewhere [10].

XUV excitation spectra were produced by 1 XUV + 1 UV resonance-enhanced two photon ionization. In such a process a highly excited bound state of CO is populated after resonant absorption of an XUV photon and subsequently ionized after nonresonant absorption of an additional UV photon. The interaction region was located between two capacitor plates with a static electric field of 100 V/cm in order to extract the ions into a 20 cm long time-of-flight (TOF) tube. The ions were detected with an electron multiplier. The signal was integrated

using a boxcar integrator and stored on a computersystem (SUN) as a function of the fundamental laser wavelength. The resolution of the TOF mass-spectrometer was in principle sufficient to separate signals from ionized species at mass 28 and 29. As no enriched  $^{13}\text{CO}$  samples were available all measurements of  $^{13}\text{CO}$  spectra were obtained from natural CO gas with 1%  $^{13}\text{CO}$ . Consequently the  $^{12}\text{CO}$  resonances were about two orders of magnitude more intense and as a result  $^{12}\text{CO}$  features could not be completely discriminated in  $^{13}\text{CO}$  spectra.

The UV light was generated by frequency doubling in a  $\text{KD}^*\text{P}$  crystal the fundamental radiation of a quanta ray PDL3 Rhodamine dye laser ( $0.07\text{ cm}^{-1}$ ) pumped by an injection-seeded Nd:YAG laser (quanta ray, GCR4). Typical UV-powers were 25 to 35 mJ. To avoid asymmetric power broadening in the CO spectra observed, only 10 to 15 mJ ultraviolet was used. This was usually sufficient to record well-resolved spectra with good signal-to-noise. From studies by Lago [11] a XUV power of about  $10^9$  photons per pulse ( $\sim 5\text{ ns}$ ) at 15 mJ UV may be estimated. Narrowband coherent radiation between 94 and 97 nm was generated.

From measurements on  $\text{N}_2$  lines [12] the bandwidth of the XUV spectrometer was determined to be  $0.36\text{ (4) cm}^{-1}$  full width half maximum (FWHM). Because of harmonic generation it was possible to calibrate the XUV spectra against a wavelength standard in the visible. With a fraction of the fundamental dye laser light an  $\text{I}_2$ -absorption spectrum was recorded simultaneously with the CO XUV excitation spectrum. By using computerized interpolation methods and the Iodine atlas, which has an absolute accuracy of  $0.002\text{ cm}^{-1}$  [13, 14] XUV frequencies may in principle be calibrated within  $0.012\text{ cm}^{-1}$ . The experimental accuracy is limited by linewidths in the spectra of both the fundamental ( $\text{I}_2$ ) and the sixth-harmonic frequency (CO) and, in weak lines, by the signal-to-noise ratio. The accuracy in the CO line positions was determined from the spread in a multitude of observations and vary between  $0.04$  (strong unblended lines) and  $0.15\text{ cm}^{-1}$  (weak lines).

### 3. Results.

**3.1 SPECTROSCOPY.** — In figure 1 a 1 XUV + 1 UV photoionization spectrum of the  $\text{K } ^1\Sigma^+ - \text{X } ^1\Sigma^+ (0,0)$  band of "hot"  $^{12}\text{CO}$  recorded in the wavelength range 96.97–97.12 nm is shown. The K-X (0,0) transition consists of an open structured line pattern without bandhead. This is typical for a  $^1\Sigma - ^1\Sigma$  transition with nearly equal rotational constants in ground and excited states. Individual and unblended rotational lines are distinguishable up to  $J = 20$  in both P and R branches. The observed intensity pattern reflects a Boltzmann population distribution over rotational states with a rotational temperature of about 250 K. Underneath the XUV excitation spectrum in figure 1 an  $\text{I}_2$  absorption spectrum recorded at the fundamental wavelength of the dye laser is also shown. For both spectra the resonances were fitted to Gaussian profiles (by computer) and the peak positions determined. In the case of the  $\text{I}_2$ -spectrum unblended and symmetrical lines were selected. Frequency positions of CO resonance were determined by interpolation between selected  $\text{I}_2$ -resonances, multiplying the result by a factor of six. Frequency scans were linearized by fitting a spline-function through a manifold of selected  $\text{I}_2$ -lines. In table I the obtained positions for K  $^1\Sigma^+ - \text{X } ^1\Sigma^+ (0,0)$  transitions for  $^{12}\text{CO}$  are listed. The quoted uncertainties in transition frequencies were determined from the spread in several measurements (in most cases six) for each resonance.

In the same wavelength range a spectrum of the K-X (0,0) band for  $^{13}\text{CO}$  was also observed. For this purpose a supersonically cooled beam with a high population density of low  $J$ -states was used. The molecular beam contains natural CO with 1%  $^{13}\text{CO}$ . For the recorded spectrum shown in figure 2 the gated TOF-mass selector was set at mass 29. As a result the weak  $^{13}\text{CO}$  resonances could be separated from the more intense  $^{12}\text{CO}$  lines. However, due to imperfect

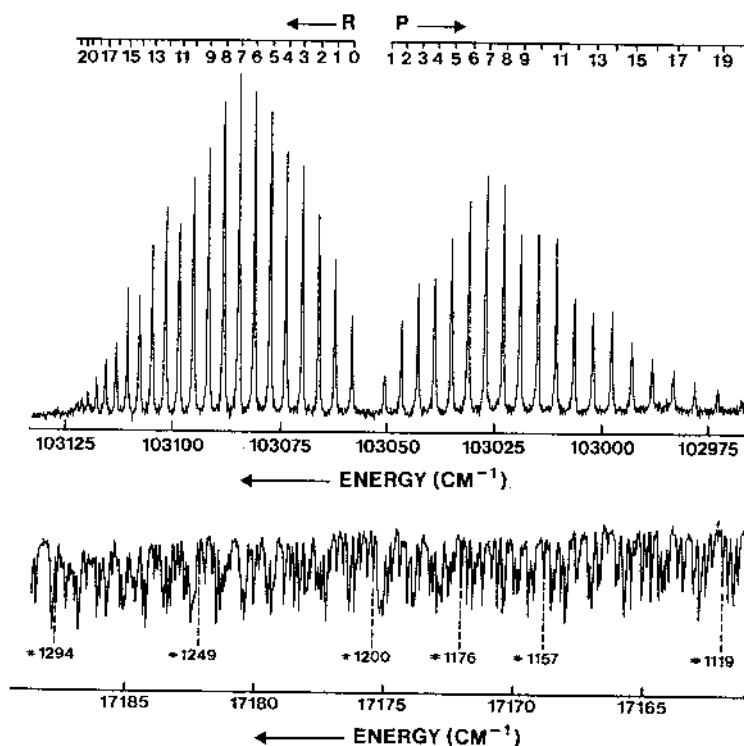


Fig. 1. — Upper part: 1 XUV + 1 UV resonance-enhanced two-photon ionization spectrum of the  $K \ ^1\Sigma^+ - X \ ^1\Sigma^+ (0,0)$  transition in  $^{12}\text{CO}$  observed in a molecular beam of near room temperature rotational distribution. Lower part:  $\text{I}_2$ -absorption spectrum recorded in the visible. Some of the unblended and symmetrical  $\text{I}_2$ -lines used for the calibration are marked with (#). Reference is made to numbers in the  $\text{I}_2$ -atlas.

mass-resolution of the TOF-setup the  $^{12}\text{CO}$  lines were not completely suppressed but show up with an intensity comparable to the  $^{13}\text{CO}$  lines. The spectrum of figure 2 shows that in the P-branch the lines of  $^{12}\text{CO}$  and  $^{13}\text{CO}$  overlap within the linewidth of about  $0.45 \text{ cm}^{-1}$ . As no additional broadening is observed due to this blending of lines it is concluded that the isotopic shift in the P(1) and P(2) lines is less than  $0.1 \text{ cm}^{-1}$ . A comparison of transition frequencies in the pure  $^{12}\text{CO}$  spectra (such as in Fig. 1) and the mixed spectra for  $^{12}\text{CO}-^{13}\text{CO}$  (such as in Fig. 2) yields values for  $^{13}\text{CO}$  P-branch transitions. In the R-branch  $^{12}\text{CO}$  and  $^{13}\text{CO}$  lines are clearly separated, although the splitting is small (on the order of  $0.5 \text{ cm}^{-1}$  for R(0)). In table I the obtained line positions of the observed  $^{13}\text{CO}$  K-X (0,0) band are also listed.

The experimental line positions were fitted to a simple expression for a rotating diatomic molecule in a  $^1\Sigma$  state:

$$E_{\Sigma} = \nu_0 + BJ(J+1) - DJ^2(J+1)^2 \quad (1)$$

where  $\nu_0$  denotes the band origin and  $B$  and  $D$  are the rotational and centrifugal distortion constant respectively. The energies of the  $X \ ^1\Sigma^+ v = 0$  ground state of  $^{12}\text{CO}$  were calculated from the accurate rotational constants of Guelachvili *et al.* [15]. From a least squares minimization routine (converging with a normalized  $\chi^2$  of 1.0) spectroscopic constants for the  $K \ ^1\Sigma^+ v = 0$  state as listed in table II were derived. As for the  $^{13}\text{CO}$  molecule only a few lines were observed the rotational constants as determined by Eidelsberg and Rostas [3] were

Table I. — Observed line positions and differences between observed and calculated positions of the  $K^1\Sigma^+ - X^1\Sigma^+ (0,0)$  band for  $^{12}\text{CO}$  and  $^{13}\text{CO}$ .  $^{13}\text{CO}$  transitions are marked with an asterisk(\*). Because of overlap with the  $^{12}\text{CO}$  lines the uncertainty in the  $^{13}\text{CO}$  line positions is  $0.15\text{ cm}^{-1}$ .

J	R(J)		P(J)	
	observed	obs.-calc.	observed	obs.-calc.
0	103058.52 (4)	-0.03		
0	*103058.00 (15)	-0.16		
1	103062.40 (4)	0.04	103050.86 (4)	-0.01
1	*103061.73 (8)	-0.02	*103050.80 (15)	-0.05
2	103066.23 (4)	0.06	103047.00 (4)	-0.01
2	*103065.33 (8)	0.03	*103047.06 (15)	-0.07
3	103070.02 (4)	0.08	103043.12 (4)	-0.02
3	*103069.00 (15)	0.19	*103043.22 (15)	-0.15
4	103073.60 (8)	-0.09	103039.28 (4)	0.03
4	*103072.49 (15)	0.22		
5	103077.32 (8)	-0.09	103035.34 (4)	0.01
6	103081.03 (4)	-0.05	103031.36 (4)	-0.04
7	103084.68 (4)	-0.04	103027.42 (4)	-0.02
8	103088.29 (4)	0.00	103023.45 (4)	0.01
9	103091.73 (4)	-0.05	103019.45 (4)	0.07
10	103095.17 (4)	-0.02	103015.30 (4)	0.03
11	103098.47 (4)	-0.04	103011.08 (4)	-0.01
12	103101.62 (8)	-0.10	103006.81 (4)	-0.02
13	103104.74 (4)	-0.04	103002.50 (4)	0.02
14	103107.73 (8)	0.02	102998.04 (4)	0.03
15	103110.59 (8)	0.12	102993.45 (4)	0.02
16	103113.15 (8)	0.12	102988.75 (4)	0.05
17	103115.39 (8)	0.01	102983.79 (4)	-0.01
18	103117.34 (10)	-0.20	102978.77 (4)	0.04
19	103119.54 (10)	0.12	102973.41 (4)	-0.04
20	103120.60 (30)	0.41	102968.00 (30)	0.06
21	103121.93 (30)	-0.37		

kept fixed. Nonetheless the high absolute accuracy of the  $\text{I}_2$ -calibration procedure allows for the determination of an accurate value for the band origin, also given in table II. The quality of the fit is apparent from the differences between experimental and calculated line positions in table I.

In figure 3 spectra of the  $W^1\Pi - X^1\Sigma^+ (2,0)$  transition recorded in the wavelength range 94.11 – 94.12 nm for  $^{12}\text{CO}$  and 94.16 – 94.17 nm for  $^{13}\text{CO}$  are presented. Again the  $^{13}\text{CO}$

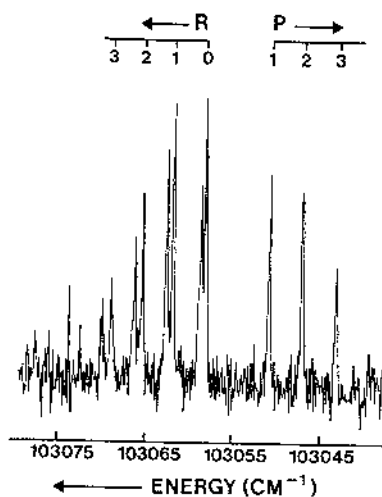


Fig. 2. — XUV excitation spectrum of the  $K \ ^1\Sigma^+ - X \ ^1\Sigma^+ (0,0)$  band in a cold beam of CO with the TOF-mass selector set at mass 29.  $^{13}\text{CO}$  peaks are marked by R and P rotational numbers. The unmarked peaks belong to the R-branch of  $^{12}\text{CO}$ . The P transitions of  $^{12}\text{CO}$  coincide with those of  $^{13}\text{CO}$ .

Table II. — Spectroscopic constants for the  $K \ ^1\Sigma^+$ ,  $v = 0$  state of  $^{12}\text{CO}$  and  $^{13}\text{CO}$ . Values marked with an (a) are taken from Eidelsberg and Rostas [3] and were kept fixed in the minimization routine.

$^{12}\text{C}^{16}\text{O}$		$^{13}\text{C}^{16}\text{O}$	
this work	Eidelsberg and Rostas [3]	this work	Eidelsberg and Rostas [3]
$B$	1.9159 (2)	1.91664 (27)	(a) 1.8174 (36)
$D$	$5.85 (6) \times 10^{-5}$	$6.0 (1) \times 10^{-5}$	(a) $2.0 (1.0) \times 10^{-5}$
$\nu_0$	103054.71 (1)	103054.07 (2)	103054.53 (4) 103053.2 (1)

features could only be discriminated from the background in a cold CO expansion with population density concentrated in the lowest rotational states. For this W-X (2,0) transition the isotope shift between  $^{12}\text{CO}$  and  $^{13}\text{CO}$  is  $54.4 \text{ cm}^{-1}$  so that the spectra are well separated. Although the  $^{13}\text{CO}$  spectrum was recorded with a poorer signal-to-noise ratio, the difference in linewidth in spectra of the isotopic species of CO was nevertheless clear.  $^{12}\text{CO}$  resonances were broader than  $^{13}\text{CO}$  lines.

The W-X (2,0) band of  $^{12}\text{CO}$  was also observed in a molecular beam with a higher rotational temperature. A recording of the spectrum, shown in figure 4, reveals the congested R-branch bandhead. In the open structured Q and P branches several lines coincide, e.g. Q(5) and P(2). Positions of the W-X (2,0) lines, as determined from repeated recordings of "warm" and "cold" spectra, are listed in table III. Line positions in blended features were deconvoluted resulting in slightly larger uncertainties. Spectroscopic constants for the excited W  $^1\Pi$  state were derived from a fitting routine using an energy expression for the  $^1\Pi$  state identical to that of the  $^1\Sigma$  state (Eq. (1)). So A-doubling effects were ignored. For the  $^{13}\text{CO}$  isotope again

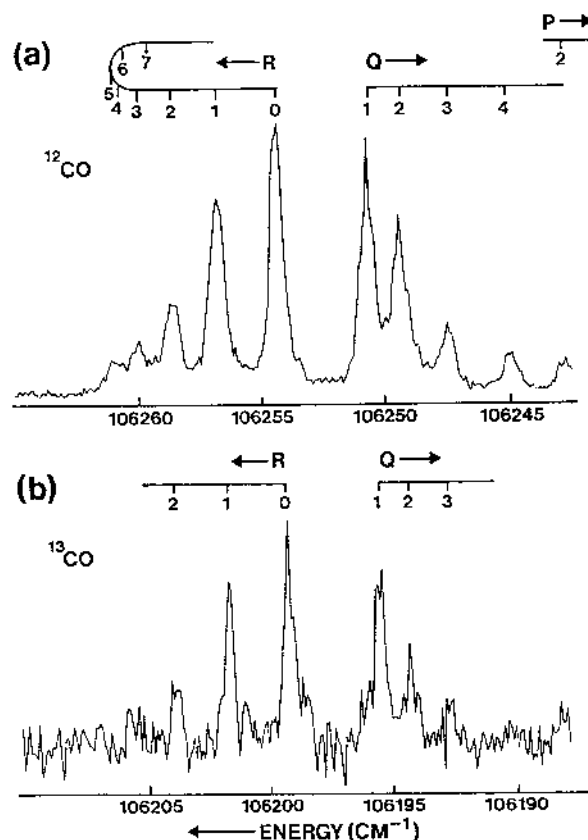


Fig. 3. —  $^{12}\text{CO}$  (a) and  $^{13}\text{CO}$  (b) spectrum of the  $W^1\Pi - X^1\Sigma^+$  (2,0) transition in a cold molecular beam. Notice the different linewidths of the  $^{12}\text{CO}$  and  $^{13}\text{CO}$  lines.

only the band origin parameter was varied and the rotational constants fixed at the values derived by Eidelsberg and Rostas, who used the same energy expression (Eq. (1)) [3]. The resulting constants with their errors are listed in table IV. Differences between experimental and calculated line positions are included in table III.

**3.2 PREDISSOCIATION.** — In excitation of various states of  $^{12}\text{CO}$  and  $^{13}\text{CO}$  different spectral widths were observed for series of unblended rotational lines. Broadening effects leading to a spectral width larger than that of the XUV radiation may be caused by fast predissociation of the excited state. In a previous experiment [12] spectral lines of  $\text{N}_2$  were observed in the same setup with a width (FWHM) of  $0.36(4) \text{ cm}^{-1}$ . The line profiles were found to be of Gaussian shape. Although the states of  $\text{N}_2$  studied ( $c'_4^1\Sigma_v^+$ ,  $v = 0$  and  $b'^1\Sigma_v^+$ ,  $v = 1$ ) are also slightly predissociating the estimated lifetimes of these states [16] preclude observable line broadening at this level of resolution. So it is assumed that the spectrometer bandwidth of the XUV laser setup was  $0.36 \text{ cm}^{-1}$ . This width was predominantly caused by the actual spectral width of the XUV radiation. The shapes of unblended rotational lines of CO in repeated scans were carefully examined and linewidths determined. Values for observed widths in excitation to the  $K^1\Sigma^+$ ,  $v = 0$  and the  $W^1\Pi$ ,  $v = 0$  and 2 states are listed in table V. Widths of



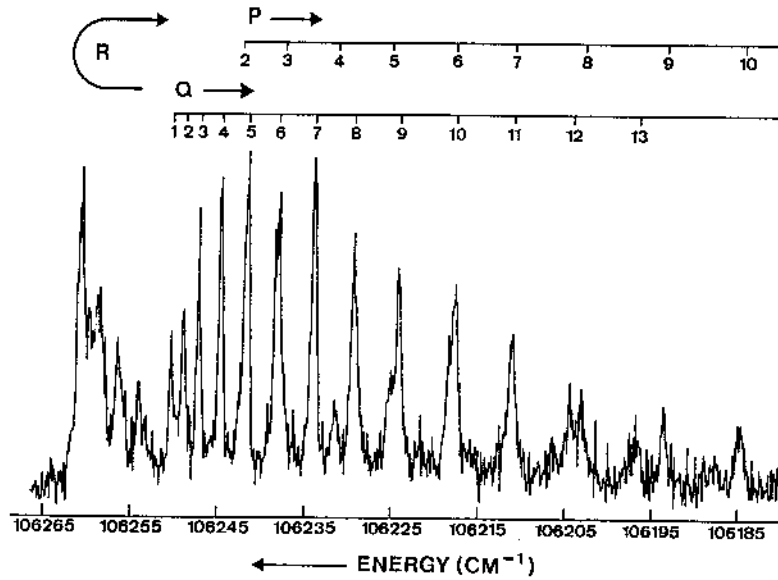


Fig. 4. — The  $W^1\Pi - X^1\Sigma^+$  (2,0) transition in  $^{12}\text{CO}$  in a “hot” molecular beam.

different rotational lines in a band were averaged; no systematic  $J$ -dependences occurred. Even the narrowest lines observed, those in excitation to the  $K^1\Sigma^+$ ,  $v = 0$  state, are slightly but systematically broader than the instrumental width. This indicates that all excited states investigated here predissociate, with a rate equal to or larger than  $10^{10} \text{ s}^{-1}$ . Effect of the radiative lifetime of the excited state may be neglected, because the states under consideration effectively predissociate for 99% [3]. Assuming a value of  $\delta\nu_{\text{instr}} = 0.36(4) \text{ cm}^{-1}$  for the instrumental linewidth an intrinsic linewidth  $\Gamma$  was deconvoluted from the observed widths  $\delta\nu_{\text{obs}}$  using the expression [17]:

$$\Gamma = \delta\nu_{\text{obs}} - (\delta\nu_{\text{instr}})^2 / \delta\nu_{\text{obs}} \quad (2)$$

The deconvolution procedure is valid with a reasonable accuracy under the conditions that  $\delta\nu_{\text{instr}}$  relates to a Gaussian and  $\Gamma$  to a Lorentzian lineprofile. Predissociation lifetime  $\tau$  and rate  $k_p$  were calculated from  $\Gamma$  using:

$$k_p = \tau^{-1} = 2\pi\Gamma c \quad (3)$$

Values for  $k_p$  and  $\tau$  are also listed in table V.

To conclude this analysis some remarks on possible experimental effects and artefacts that might influence the observed linewidth in spectra recorded with the technique of 1 XUV + 1 UV two-photon ionization are appropriate. In a previous experiment [12] power broadening effects were observed in excitation of the  $c'_4^1\Sigma_u^+$ ,  $v = 0$  state of  $\text{N}_2$ , that is known to have a large oscillator strength and a marginal ( $\sim 10\%$ ) predissociation [16]. For the strongly predissociating levels of CO no significant effects of XUV or UV input powers were found. Residual Doppler widths due to laser and molecular beam divergencies (on the order of  $0.02 \text{ cm}^{-1}$ ) were included in the instrumental width. Furthermore the UV ionizing radiation may cause population depletion of the excited state and therewith shorten its lifetime. With the use of

Table III. — Observed line positions in the  $W^1\Pi - X^1\Sigma^+ (2,0)$  band for  $^{12}\text{CO}$  and  $^{13}\text{CO}$  (with asterisk (\*)). The positions of  $^{13}\text{CO}$  lines are slightly less accurate due to poorer signal-to-noise ratio. Differences between observed and calculated line positions are also included. Blended lines are marked with (b). Lines marked with (a) were not used in the minimization routine because of large uncertainties.

$J$	R( $J$ )		Q( $J$ )		P( $J$ )	
	Observed	obs.-calc.	observed	obs.-calc.	observed	obs.-calc.
0	106254.15 (8)	0.09				
0	*106199.36 (10)	-0.13				
1	106256.69 (8)	-0.02	106250.37 (10)	0.15		
1	*106201.93 (10)	-0.03	*106195.75 (10)	-0.06		
2	106258.60 (10)	-0.17	106249.02 (8)	-0.01	106242.69 (10)	0.16
2	*106204.08 (15) <sup>(b)</sup>	0.25	*106194.64 (10)	0.04		
3			106247.23 (8)	0.00	106237.53 (10)	0.04
3			*106192.96 (15) <sup>(b)</sup>	0.16		
4			106244.80 (8)	-0.05	106231.73 (10)	-0.13
5			106241.84 (10)	-0.03	106225.28 (30) <sup>(b)</sup>	-0.35
6			106238.24 (10)	-0.06	106218.02 (50) <sup>(b)</sup>	-0.79
7			106234.10 (8)	-0.02	106211.34 (20) <sup>(b)</sup>	-0.05
8			106229.49 (8)	0.14	106203.11 (20) <sup>(b)</sup>	-0.26
9			106224.19 (30) <sup>(b)</sup>	0.21	106193.82 (50) <sup>(a),(b)</sup>	-0.94
10			106218.02 (50) <sup>(b)</sup>	-0.00	106185.07 (50) <sup>(a),(b)</sup>	-0.49
11			106211.34 (20) <sup>(b)</sup>	-0.11		
12			106204.35 (20) <sup>(b)</sup>	0.05		
13			106196.85 (50) <sup>(a),(b)</sup>	0.32		

Table IV. — Spectroscopic constants for the  $W^1\Pi, v = 2$  state of  $^{12}\text{CO}$  and  $^{13}\text{CO}$ . Values marked with an (a) are taken from Eidelsberg and Rostas [3] and were kept fixed in the minimization routine.

	$^{12}\text{C}^{16}\text{O}$		$^{13}\text{C}^{16}\text{O}$	
	this work	Eidelsberg and Rostas [3]	this work	Eidelsberg and Rostas [3]
$B$	1.6246 (8)	1.6260 (27)	(a)	1.5370 (26)
$D$	(a)	$7.7 (8) \times 10^{-6}$	(a)	$5.0 (3.0) \times 10^{-6}$
$\nu_0$	106250.81 (3)	106249.9 (2)	106196.41 (5)	106195.7 (5)

diverging laser beams in the interaction zone this effect is estimated to be of minor importance. The dependence of the linewidths on XUV and UV intensities were carefully examined and no effects observed in the range of UV input powers between 8 – 35 mJ. It can be concluded that

Table V. — Observed linewidth  $\delta\nu_{\text{obs}}$ , and deconvoluted values for the intrinsic linewidth  $\Gamma$ , excited state lifetime  $\tau$  and predissociation rate  $k_p$  for the K  $^1\Sigma^+$ ,  $v = 0$  and W  $^1\Pi$ ,  $v = 2$  states of CO.

		$\delta\nu_{\text{obs}}(\text{cm}^{-1})$	$\Gamma(\text{cm}^{-1})$	$\tau(\text{s})$	$k_p(\text{s}^{-1})$
W $^1\Pi$ , $v = 2$	$^{12}\text{CO}$	0.78 (5)	0.61 (6)	$0.87 (9) \times 10^{-11}$	$1.15 (15) \times 10^{11}$
	$^{13}\text{CO}$	0.55 (5)	0.31 (7)	$1.7 (5) \times 10^{-11}$	$0.58 (13) \times 10^{11}$
K $^1\Sigma^+$ , $v = 0$	$^{12}\text{CO}/^{13}\text{CO}$	0.44 (4)	0.14 (7)	$3.8 (1.9) \times 10^{-11}$	$2.6 (1.3) \times 10^{10}$

the linewidths in the observed spectra are only due to bandwidth of the exciting XUV radiation and predissociation effects.

An important characteristic of the 1 XUV + 1 UV ionization scheme is that the observed line intensities depend on the lifetime of the intermediate state, at least under circumstances where its lifetime is shorter than the duration of the laser pulse ( $\sim 5$  ns). This assumption is certainly valid for the CO levels studied here. In 1 + 1 photoionization there is a competition between ionization and dissociation (with neglect of radiative decay) and the number of ions produced depends on the time a molecule spends in the excited, intermediate state. For the spectra of the W-X (2,0) band an intensity ratio for  $^{12}\text{CO}$  and  $^{13}\text{CO}$  of approximately 30 : 1 was found. For relative populations in the molecular beam of 100 : 1 this indicates that the predissociation rate of the W  $^1\Pi$ ,  $v = 2$  state of  $^{13}\text{CO}$  is smaller than that of the corresponding state of  $^{12}\text{CO}$ . From the analyses based on linewidths a factor of two was found. In view of the uncertainties in the experimental values this agrees well. So it can be concluded that the observed intensities confirm the conclusion of the isotopic dependence of lifetimes and predissociation rates.

#### 4. Discussion and conclusions.

In the present investigation a newly built XUV laser spectrometer was used for high resolution studies of the K  $^1\Sigma^+$ ,  $v = 0$  and W  $^1\Pi$ ,  $v = 2$  excited states of CO. The resolution in the present experiment was higher than in previous studies using a large 10 m spectrometer [3] or a synchrotron [5] ( $0.36 \text{ cm}^{-1}$  instead of  $0.5 \text{ cm}^{-1}$ ). The data provide new and additional information in terms of spectroscopic constants and predissociation rates. The rotational and centrifugal distortion constants found for  $^{12}\text{CO}$  in the K  $^1\Sigma^+$ ,  $v = 0$  and W  $^1\Pi$ ,  $v = 2$  states are in agreement with those found by Eidelsberg and Rostas [3]. However, values for the band origins  $\nu_0$  found by Eidelsberg and Rostas are systematically lower than the present values. The differences are  $0.64$  and  $1.3 \text{ cm}^{-1}$  for the K-X bands, and  $0.9$  and  $0.7 \text{ cm}^{-1}$  for the W-X bands for  $^{12}\text{CO}$  and  $^{13}\text{CO}$  respectively. The simultaneous recording of the  $\text{I}_2$ -reference standard and the XUV excitation spectrum at the sixth harmonic frequency has the advantage that many rotational transitions in the XUV range are calibrated with an absolute accuracy of  $0.04 \text{ cm}^{-1}$ . The discrepancy in band origin values is probably due to the difficulty in the absolute calibration of classical absorption studies.

The determination of accurate absolute transition frequencies in both  $^{12}\text{CO}$  and  $^{13}\text{CO}$  may have important consequences for the modelling of the XUV induced photodissociation dynamics in outer space [2]. Shielding effects by H atoms and  $\text{H}_2$  molecules and their isotopes are influenced by the frequency differences with the absorption lines of carbon monoxide and hydrogen. Mutual shielding effects of  $^{12}\text{CO}$  and  $^{13}\text{CO}$  resonances are equally important. In this respect the simultaneous recording of  $^{12}\text{CO}$  and  $^{13}\text{CO}$  features in a spectrum as shown in

figure 2 for the  $K \ ^1\Sigma^+ - X \ ^1\Sigma^+ (0,0)$  transition bears relevance. The low  $J$ -state P-branch lines in this band perfectly overlap for both isotopes, while the R-lines are resolved. The effective mutual shielding on these lines will critically depend on the ratio  $^{12}\text{CO}/^{13}\text{CO}$ , the Doppler width in the environment considered (which depends on the velocity of the medium with respect to neighbouring stellar XUV sources as well as on temperature), and on the presently obtained isotope shifts for the R( $J$ ) lines. These shifts have not yet been incorporated in the sophisticated model calculations for interstellar regions [1,6].

Values for the lifetimes of the  $K \ ^1\Sigma^+$ ,  $v = 0$  and  $W \ ^1\Pi$ ,  $v = 2$  excited states of CO were reported previously. The lifetime of the  $K$ ,  $v = 0$  state was estimated to be  $10^{-10}$  s and that of the  $W$ ,  $v = 2$  state  $10^{-11}$  s for both isotopic species [3,6]. Due to the higher resolution more accurate values for lifetimes and predissociation rates were obtained in the present investigation. Nevertheless the agreement is satisfactory in view of the uncertainties in the earlier values.

The isotopic dependence of the predissociation rate for the  $W \ ^1\Pi$ ,  $v = 2$  state is quite significant. The measurement of relative line intensities in 1 + 1 two-photon ionization spectra support the conclusion of different rates of predissociation for  $^{12}\text{CO}$  and  $^{13}\text{CO}$ . In itself an isotopic dependent predissociation rate is not new. For example a remarkable difference for the rates of  $^{12}\text{C}^{16}\text{O}$  and  $^{12}\text{C}^{18}\text{O}$  was found for the  $4s\sigma \ ^1\Sigma^+$  state excited at 98.6 nm [3]. However, the  $W \ ^1\Pi$ ,  $v = 2$  state was found to play an important role in the isotope dependent fractionation of CO [1,2] in interstellar matter at specific column densities. Although for both  $^{12}\text{CO}$  and  $^{13}\text{CO}$  the branching ratio for dissociation is larger than 99% a difference in predissociation rate of a factor 2 to 3 may still have an impact, particularly at high column densities such as in the centers of interstellar clouds.

Although the method of 1 XUV + 1 UV two-photon ionization using narrow band XUV laser radiation has certain advantages, it is nevertheless complementary to direct absorption measurements. The higher resolution in the present experiment allows for quite accurate determination of lifetimes in the range  $10^{-10}$  to  $10^{-11}$  s. An advantage of the molecular beam setup is that a small interaction volume eliminates column density or pressure saturation effects that are known to disturb absorption studies [4]. But most of all the achieved absolute accuracy in the transition frequencies in the laser experiment is an improvement. However, the 1 XUV + 1 UV detection scheme can not provide reliable information on photoabsorption cross sections. In this respect the classical absorption studies of Eidelsberg and Rostas [3] and Stark *et al.* [5] are important.

The resolution in the present experiment is only limited by the band width of the dye laser. In the near future the bandwidth of the XUV spectrometer will be reduced by replacing the multi-mode by a single-mode pulsed dye laser.

#### Acknowledgements.

The authors wish to thank E. van Dishoeck for stimulating discussions. We thank J. Bouma for his technical support with the construction of the XUV-laser source and K. Eikema for his assistance during measurements and interpretation of data. Financial support from the Foundation for Fundamental Research on Matter (FOM) and the Netherlands Organisation for the Advancement of Research (NWO) is gratefully acknowledged.

## References

- [1] VAN DISHOECK E.F., *Rate Coefficients in Astrochemistry*, T.J. Miller and D.A. Williams Eds. (Kluwer Academic Publishers, 1988) p. 49.
- [2] VAN DISHOECK E.F. and BLACK J.H., *Astrophys. J.* **334** (1988) 771.
- [3] EIDELBERG M. and ROSTAS F., *Astron. Astrophys.* **235** (1990) 472.
- [4] LETZELTER C., EIDELBERG M., ROSTAS F., BRETON J. and THIEBLEMONT B., *Chem. Phys.* **114** (1987) 273.
- [5] STARK G., YOSHINO K., SMITH P.L., ITO K. and PARKINSON W.H., *Astrophys. J.* **369** (1991) 574.
- [6] VIALA Y.P., LETZELTER C., EIDELBERG M. and ROSTAS F., *Astron. Astrophys.* **193** (1988) 265.
- [7] HOSOI N., EBATA T. and ITO M., *J. Phys. Chem.* **95** (1991) 4183.
- [8] HINES M.A., MICHELSEN H.A. and ZARE R.N., *J. Chem. Phys.* **93** (1990) 8557.
- [9] MASAKI T., ADACHI Y. and HIROSE C., *Chem. Phys. Lett.* **139** (1987) 62.
- [10] LEVELT P.F., EIKEMA K., UBACHS W. and HOGERVORST W., to be published.
- [11] LAGO A., Ph.D. Thesis, University of Bielefeld, Germany (1987).
- [12] LEVELT P.F. and UBACHS W., *Chem. Phys.*, accepted for publication.
- [13] GERSTENKORN S. and LUC P., *Atlas du spectre d'absorption de la molécule de l'iode entre 14800 - 20000 cm<sup>-1</sup>* (Editions du CNRS, Paris, 1978).
- [14] GERSTENKORN S. and LUC P., *Revue Phys. Appl.* **14** (1979) 791.
- [15] GUELACHVILI G., DE VILLENEUVE D., FARRENQ R., URBAN W. and VERGES J., *J. Mol. Spectr.* **98** (1983) 64.
- [16] AJELLO J.M., JAMES G.K., FRANKLIN B.O. and SHEMANSKY D.E., *Phys. Rev. A* **40** (1989) 3524.
- [17] DOBRYAKOV S.N. and LEBEDEV Y.S., *Sov. Phys. Dokl.* **13** (1969) 873.